STAARK - Affordable and Mission-Agnostic Robotic Arm

Vinayak Vadlamani, Menelaos Vidakis, Dr. Jan Dentler, Jaroslaw Jaworski, Dr. Serket Quintanar-Guzmán, Benjamin Favier, Aurélie Bressollette, Nicholas Parrotta

Redwire Space Luxembourg

According to Space Robotics Market Report, 2027 GTP [1], the market for space robotic manipulators will reach 309 mil EUR in 2023, with an average CAGR of 5.8% until 2032. This market growth is particularly driven by in-orbit satellite servicing, manufacturing, and assembly missions. However, a crucial gap exists in the availability of affordable space robotic manipulators and space business cases. Recognizing this opportunity, Redwire established a subsidiary in Luxembourg focusing on space robotics. Since 2019 this entity developed and commercialized an off-the-shelf space-grade robotic system family named "STAARK", under the Luxembourg Space Agency national program, "LuxImpulse". STAARK's focus is on modular design that seamlessly integrates into various spacecraft platforms and mission concepts with minimal costs.

1. INTRODUCTION

The research and development process of STAARK spans from customer hypothesis verification, system requirements definition, design, and testing, up to system qualification. Redwire leverages proven robotic knowledge to iteratively extend STAARK's capabilities through rapid development intervals. Reliability and performance are thereby ensured with advanced simulation tools, software frameworks, and process automation, combined with extensive physical testing.

The work presented here introduces STAARK's development philosophy, specifications, features, and capabilities. It highlights the development process, concepts for control, modularity, autonomy, and the key challenges encountered. It elaborates on the qualification process and results, demonstrating STAARK's performance, and reliability. Finally, concludes with major lessons learned and discusses the future path of STAARK.

2. MISSION ANALYSIS AND REQUIREMENTS

Space robotic arms have a number of applications ranging from RPO operations (docking) to target tracking and capturing, on-orbit servicing and in-orbit assembly, pressurized-depressurized space station automation to inspections.

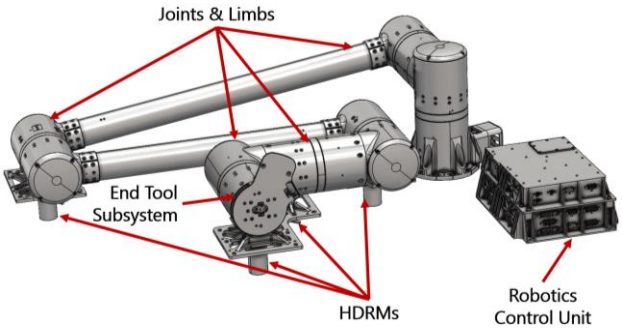

Figure 1: STAARK LEO Small Robotic System Configuration.

These applications are relevant to a range of vehicles and orbits, from small satellites in LEO to large structures in GEO.

Table 1: STAARK LEO Small Requirements.

Title:	Requirement:
Reach	The robotic arm shall have a minimum reach, when fully extended, of 1.5 meters.
Dexterity	The STAARK robotic arm shall have at least 6 degrees of freedom.
Maximum Mass	The maximum mass of the robotic arm, without the gripper, shall not be more than 40 kg.
Teleoperations	The robotic arm shall be capable of teleoperation through telecommands via a ground control interface.
Stowage	The robotic arm shall have a stowed volume of 1000 x 700 x 300 mm^3.
Lifetime	The robotic arm shall exceed an on-orbit life of 5 years in LEO environment.
Positioning Accuracy	The robotic arm shall have a positioning accuracy of 5 mm at its tip.
Force-Torque Capability	The robotic arm shall have the capability to output 100 N and 100 Nm at its tip when operating in LEO.
Arm Control	The robotic arm shall be capable of cartesian position and speed control level.
Joint Control	The robotic arm shall be capable of independent joint position control.

Redwire has identified industry trends and prevalent configurations across various applications through comprehensive market research. This insight has guided the conceptualization of a versatile range of robotics modules and families, which can be flexibly combined to achieve diverse configurations.

Based on the highest and most immediate demand, Redwire started with the initial product "STAARK LEO Small" in the context of a LuxImpulse R&D grant, as illustrated in Figure 1 and Table 1. STAARK LEO Small is a 6 degree of freedom (DOF) manipulator designed for teleoperation and semiautonomous operations in low-earth orbit (LEO), such as handling, un/loading, inspection and assembly tasks.

3. DESIGN PHILOSOPHY

The STAARK robotics family was designed to leverage economy of scale in a new space design approach, hence, the focus is low single item costs and adaptability to most business cases. In combination with the mission context this introduces challenging objectives, such as low part costs, low mass, low power consumption, high system reliability, high system configurability/flexibility and high system autonomy. During development Redwire adopted a philosophy that focused on:

- Leveraging existing solutions where possible, domain experts' knowledge and external reviews
- Rapid iterative development with focus on early and extensive testing, automation of processes and infrastructure
- Building inhouse test facilities
- Creating lists of preferred parts & screened suppliers
- Utilizing COTS where possible according to risk analysis with a focus on space heritage

4. SYSTEM DESIGN & CONFIGURATION

STAARK is designed as a product for worst case space environmental loads and qualification requirements. Figure 1 shows the current configuration of the STAARK system.

It consists of two shoulder joints, one elbow joint in an offset limb configuration for easier stowage, and three wrist joints. For simplicity and to maintain low cost, six identically rated joints are currently used, which will be complemented by smaller wrist joints in the future. Each joint is controlled locally by the internal joint control system. The collection of joints is managed by a Robotic Control Unit (RCU) responsible for path planning, power distribution, and interfaces to the customer. Internal harness connects the joints and end effector through a communication and power bus. The external structure is covered by a special coating to achieve the desired thermal properties. Table 2 shows the main specifications of the current STAARK configuration.

Table 2: STAARK LEO Small Specification Overview.

Property:	**Value:**
Manipulator Mass	35.4 kg
Spacecraft Subassemblies Mass	4.1 kg
Reach	1.965 m
Dexterity	6 DOF
Stowage Volume	994mm x 652mm x 273mm
Joint Torque Rating	220 Nm
Max Tip Speed	25 mm/s (adjustable)
Max Manipulatable Mass	1900 kg at 10 mm/s^2 max acceleration
Communication Interface	Space Packet Protocol: 1xRS422 – Supervisor 1xRS422 – Application 1xEthernet – Perception
Control Features	Onboard task automation pipeline, Cartesian/joint space control, path planning with static collision detection, visual servoing & compliance control with additional sensors
Manipulator power	28V power: - Main power - Redundant power - Survival power
End effector data interface	1 x 28V power line 4 x GPIO 1 x CAN interface
Joint Control Accuracy	0.05 deg
Operating Temperature	-30C to +50C
Survival Temperature	-40C to +60C
EMI / EMC	MIL-STD-461
Quasi Static Loads	25 g X, Y, Z
Sine Loads	25 g X, Y, Z 0-100 Hz
Random Loads	15.3 GRMS., X, Y, Z 0-2000 Hz

The current baseline configuration of STAARK includes the following subsystems:

1. The arm is an offset limb, non-spherical wrist joint, Yaw-Pitch-Pitch-Pitch-Roll-Yaw configuration and has two round aluminum section booms, with

interfaces to lock the motion of the joints during launch.

2. The mechanical interface subsystem consists of a sensor suite with a vision sensor, a standardized tool flange interface for power, data and mechanical connections to service a third-party end effector (EE).
3. The Hold Down and Release Mechanisms (HDRM) set consists of four active Frangibolt based resettable low-shock separation actuators.
4. The RCU consists of a processing platform, power conditioning, and customer interfaces.
5. The flight harness set includes an internally routed harness with slack management to serve the joints and EE, as well as an external harness connection between manipulator and RCU.
6. The flight software is composed of the high-level Manipulator Control Stack (MACOS) and low-level firmware, such as Robotics Control Unit Supervisor firmware (RCUS) and low-level joint control system (JCS) firmware.

4.1. Joint Design Overview

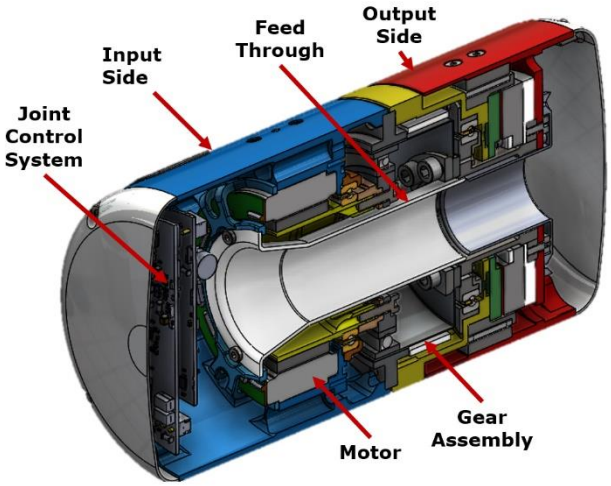

Figure 2: STAARK Joint Design.

The joint design is driven by modularity and performance and is based on a rotary hollow shaft motor and strain wave gearset to allow for internal harness routing. It includes modular housing, and motion controller boards. Figure 2 shows the design architecture of the current joint baseline.

In more detail the design of the joint is based on:

- Motor – Brushless direct current motor with space heritage
- Gear assembly – Strain wave gearset based on space mechanisms heritage, thin section and needle bearings.
- Feed through for harness routing.
- Input Sensors – Magneto-resistive based position sensor for input rotor incremental position feedback (space grade version currently under development).
- Output Sensors – Absolute encoder based on inductive sensing.

Figure 3 shows the Joint Control System assembly consisting of the Joint Power Distribution Unit (JPDU) and the Joint Controller Unit (JCU). The JPDU is responsible for the voltage regulation, filtering, and safety supervision of the joint subsystem. The JCU is responsible for low level joint motion, sensor processing (encoders, temperature sensors) and motor control. The JCU has a cut-out to allow direct connection of the harness to the JPDU.

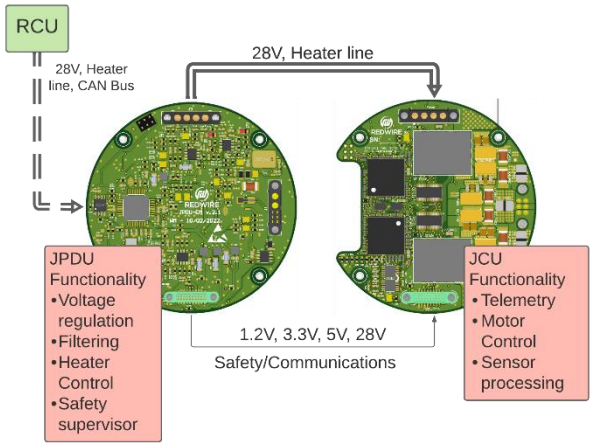

Figure 3: JCS: JPDU and JCU power & data interfaces.

4.2. Harness Design Overview

Following the completion of the electronics design and interface definition, the internal manipulator harness has been designed. Internal harnessing has been chosen based on a trade-off study, considering superior system safety and reliability. Figure 4 shows the full EQM version of the harness.

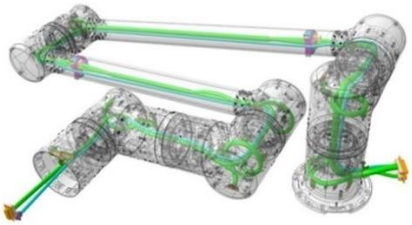

Figure 4: Internal harness integration in STAARK arm.

The internal harness begins at the arm's base joint and runs through all joints until the end effector. It provides power and communication from the base of the arm to all six joints and the end effector while also including a 1 Gbps ethernet connection for vision sensors at the tip of the arm. The key challenge of this design has been to ensure reliability and longevity in the context of motion under the given environmental conditions.

This is addressed by special wire selection for minimal bend radius under low temperatures and harness slack management. The risk of faults due to material stiffness increases for low temperatures. This risk has been mitigated via a dedicated test campaign:

- Integration test in a mock-up joint
- Twist test in thermal chamber at -30 ˚C and ambient temperature for 1000 cycles
- Twist test in thermal vacuum chamber at -30 ˚C and ambient temperature for 1000 cycles
- Flat arm continuity test.

For the twist test in a thermal chamber, a test setup was devised as shown in Figure 5. One part of the harness was fixed to the thermal chamber while the other side was clamped to the output shaft of a motor sitting outside the thermal chamber connected via a sealed feedthrough.

Figure 5: Harness Thermal Chamber twist test configuration.

A second harness mock-up was used to test under TVAC conditions for 1000 cycles. The joint used for testing was equipped with additional clamps to emulate the bending radius as would be experienced by the harness within the manipulator and reproduce the nominal slack at the joint-to-joint interface. After the tests were completed, visual inspection and continuity checks showed no material degradation of the wires.

4.3. Robotics Control Unit Design Overview

The RCU is designed to serve as an interface to the spacecraft to and from the manipulator. It contains the Robot Processing Unit (RPU) for data processing and communication, the Power Distribution Unit (PDU) for power conditioning, and an Interface PCB (IPCB), for ease of integration and customer interface flexibility. Figure 6 shows the 3D model of the RCU stack up.

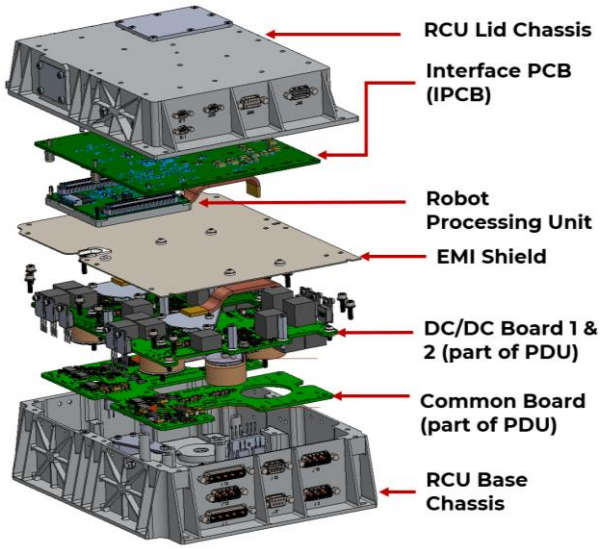

Figure 6: Robotics Control Unit architecture.

To ensure availability of system telemetry and recoverability, the critical power and communication paths in the RCU are based on high reliability components, a concept referred to as "rad hard island".

4.4. Software Architecture and Design

The STAARK software stack is developed in a heterogenous architecture to combine high autonomy with high reliability. The autonomy roadmap is illustrated in Figure 7. The focus of the STAARK development is the advanced capabilities package for 2024.

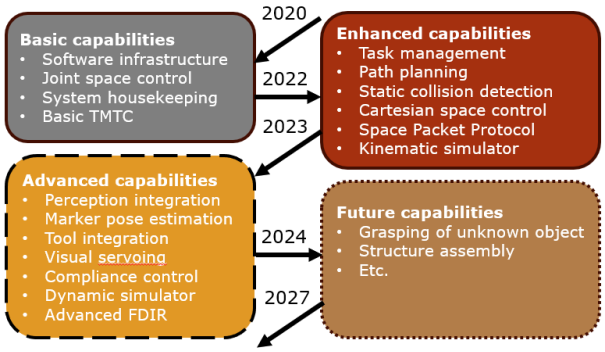

Figure 7: STAARK autonomy map.

To accommodate performance and reliability, there are two operation paths, in nominal condition, the system is operated through the application processor running MACOS for high processing performance such as on-board path planning, etc. As a fallback option, the application processor can be isolated, and the system can be commanded purely through the high reliability supervisor in joint space which is part of the "rad hard island".

Like STAARK as a product, the software is designed modularly. This facilitates local changes of drivers, features, etc. The low-level firmware is structured in software modules and follows a layer design pattern to facilitate code reuse and abstraction of the application development from drivers as far as possible.

Higher level MACOS has been developed with minimal dependencies, relying on a POSIX-compliant operating system to enable rapid development and testing while maintaining portability to different hardware and operating systems. This further allows us to scale STAARK's functionality with the next generations of flight processors.

Modularity is also used to address the concern of time determinism for a complex processing system. The functionality/modules are isolated on dedicated CPUs with defined data update frequencies, e.g., management and control of joints is handled by CPU1, the manipulator by CPU2, etc. The instructions of the modules are running on these isolated CPUs sequentially. In addition, all memory allocation is static after initialization.

To enable the use of STAARK in scenarios with unstable/limited ground communication access or scenarios with low system response times, MACOS supports onboard autonomous execution of tasks using an action framework. These actions constitute atomic behaviors that are defined by operations performed at the start, during and at the end of an action. Sequences of actions are executed autonomously via a pipeline. Additional onboard features include algebraic and biologically inspired inverse kinematics, sample-based planners, trajectory generation, static collision detection, as well as joint and Cartesian space control [2]. Additional sensors, compliance control and visual servoing using fiducial markers are also supported [3]. MACOS also provides a simulation environment for the kinematic behavior of the arm in mission context.

5. SYSTEM QUALIFICATION

The verification of the STAARK robotic system and its qualification was planned to be carried out at three levels, Joint level Qualification, Manipulator level Qualification and System level Qualification as shown in Figure 8.

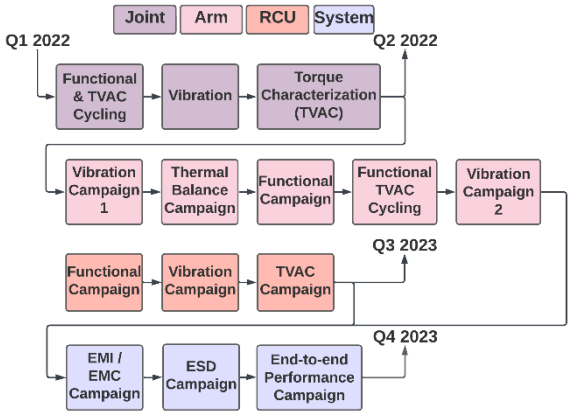

Figure 8: STAARK Verification Plan.

The STAARK LEO Small qualification started with joint qualification to TRL 6. Currently the arm, the flight harness and the HDRMs are under qualification to TRL 6 (end of 2023) while the RCU is currently at TRL 5 and undergoing qualification (end of 2023) and the flight software is at TRL 4 with qualification planned for 2024.

The STAARK qualification is as per the requirements for space segment sub-system hardware and software. In case the expected environments for a mission are more severe than the qualification environment for STAARK, the design justification will be done through appropriate analysis or delta-qualification tests.

5.1. Joint Qualification

The joint qualification consisted of TVAC cycling with functional tests in various stages of the cycle, vibration tests in various directions and joint torque characterization in TVAC.

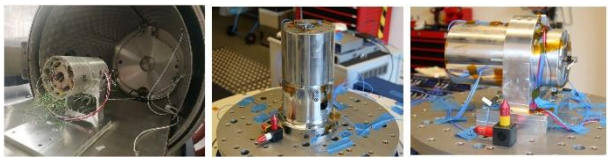

Figure 9: Left – Joint configuration in TVAC for TVAC cycling. Centre – Joint vertical configuration on shaker for vibration. Right – Joint lateral configuration for vibration.

For the TVAC Cycling & functional testing, joint functional and performance tests were carried out at different stages of the cycle to verify the stable performance of the joint while operating the joint under different run profiles. These tests are designed to monitor any deviation from nominal values in current, voltage, torque, telemetry, and temperatures on the joint components while operating within the operational range temperature limits (-30ºC, +50ºC). For this purpose, the joint was placed in TVAC with MGSE equipment in a configuration shown in Figure 9.

The test results collected from the hot and cold case functional testing are presented in Table 3. The thermal vacuum cycling campaign was conducted successfully with the joint subjected to the entire qualification temperature range. The tests revealed nominal behavior of the joint electronics, mechatronics, and lubrication that showed variation expected within such thermal range. The joint position accuracy and repeatability requirements were achieved over the full temperature range.

Table 3: Test results from joint functional testing while in TVAC cycling.

	Requirement	Reference input	Accuracy (Cold Case)	Accuracy (Hot Case)
1	Position accuracy < 0.05°	(rad) 1.0 3.0 2.0 -1.0 -3.0 -2.0	6.266E-4 rad	7.156E-5 rad
2	Position control repeatability < 0.005°	(rad) (0.0, 1.0) x 20	Repeatability: 6.702E-5 rad	Repeatability: 4.538E-5 rad
3	Range of motion < ±90°	(rad) 0, -π/2, 0, π/2	3.31E-4 rad	4.54E-5 rad
4	Velocity control stress test	rad0.0524 rad/s (0.5 rpm)	9.6E-4 rad/s	7.52E-4 rad/s
5	Velocity control stress test	0.157 rad/s (1.5 rpm)	7.69E-4 rad/s	1.97E-4 rad/s
6	Velocity control stress test	0.367 rad/s (2.2 rpm)	1.28E-3 rad/s	3.24E-3 rad/s

For the joint vibration testing two setups have been tested, as shown in Figure 9, a vertical setup with the joint in vertical position with excitation along its axial (vertical) axis and a lateral setup with the joint in lateral position with excitation along one of its lateral (vertical) axis. The results that are presented here are of the vertical orientation. The summary of modes that have been identified are presented in Figure 10. Successful sine and random vibration tests have also been conducted.

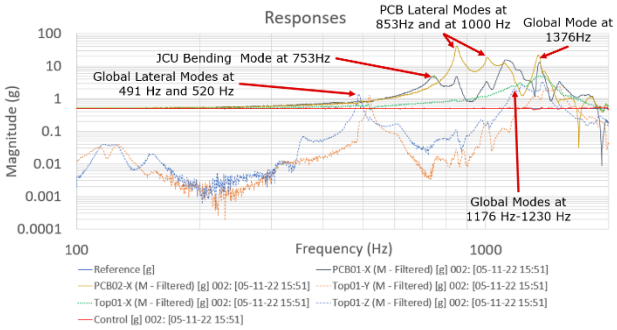

Figure 10: Joint resonance check frequency responses (magnitude – frequency).

The next step for the STAARK joint is the qualification and integration of an input shaft position sensor to enable higher speeds and torques by end of 2023. The joint characterization is going to be conducted in the TVAC with MGSE equipment and a shaft feed out of the TVAC connected to a torque break as shown in Figure 11.

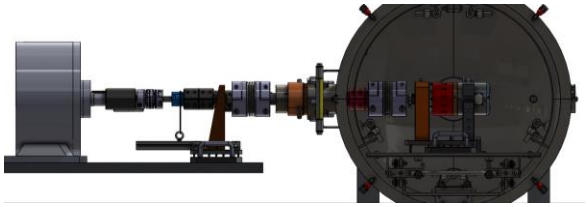

Figure 11: Joint torque characterization configuration.

5.2. Arm Qualification

The arm qualification consists of functional, performance, vibration, TVAC cycling, thermal balance, EMI/EMC, and lifetime testing.

Functional tests were performed in a flat testbed setup shown in Figure 12:

- Repeatability test in position control mode.
- Velocity mode test.
- Measure the power consumption of the joint for 10 seconds.
- Read Joint Heartbeats.
- The CAN communication test for all the joints in the EQM arm.

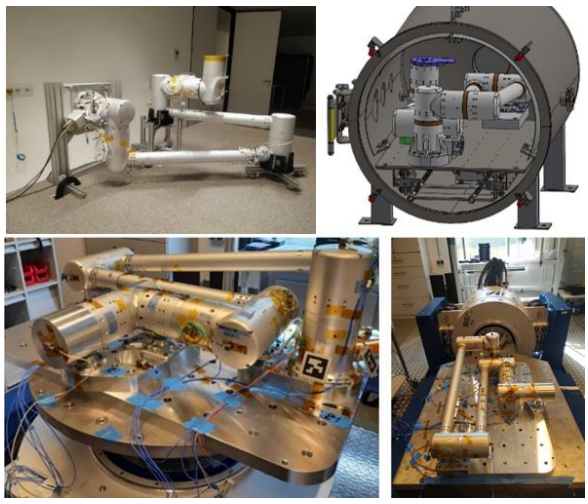

Figure 12: Top Left - Arm flatbed functional test. Top Right – Arm configuration for TVAC cycling. Bottom Left - Arm configuration for vertical vibration testing. Bottom Right - Arm configuration for horizontal vibration testing.

Figure 13 shows the position plot of the joints used in the multi-joint flatbed functional test. All the joints in the arm (except for the 1st joint) were commanded to reach position 0. Joints 2, 3 and 4 were moved to their maximum range while joints 5 and 6 were positioned to avoid any self-collision. Then, all joints were commanded simultaneously to move to position 0 at constant velocity 0.5 rpm. Since each joint had a different starting position, the position settling time differs. Figure 14 shows the overall power consumption of the arm during the duration of the motion with a peak at 50 Watt observed during the beginning of the deceleration maneuver.

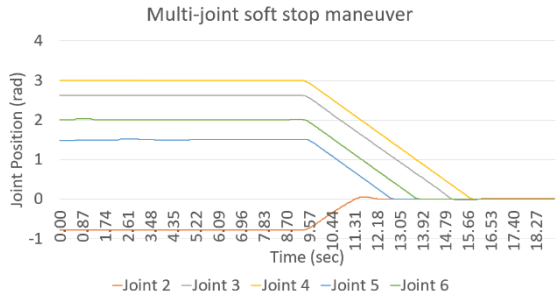

Figure 13-joint position – time graph to position 0 test data.

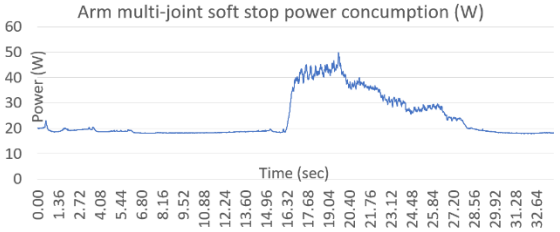

Figure 14: Arm power consumption – time during brake maneuver.

For the first vibration campaign, random and sine vibration tests were performed with resonance checks at various points throughout the campaign. The manipulator vibration test campaign was conducted via a TIRA Vib 89kN Shaker. Z Axis vibration is carried out using an 800 mm diameter head expander, whereas X and Y axis vibration is carried out on the Slip table. Figure 12 shows the system mounted on the vibrator for vertical vibration.

After the tests it was apparent that the passive HDRM did not manage to maintain the preload. Hence, the arm was qualified at a later campaign with all active HDRMs (Vib. Campaign 2). Table 4 shows the comparison between the resonance frequencies identified from the test and from the FEM model.

Table 4: Comparison between FEM and test resonance frequencies.

Resonance Frequencies (Hz)

Test	FEM
123	103
141	112
170	160
290	217

The thermal balance test was performed in order to obtain thermal data for a TMM (Thermal Math Model) correlation and verifying thermal control subsystem performance.

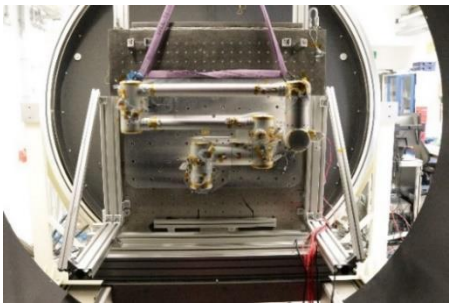

Figure 15: Arm mounted in TVAC sun simulator for thermal balance testing.

The mounting orientation, as shown in Figure 15, of the arm was selected such that the plane of arm mounting plate is normal to the sun simulator light beam. The relative placement and angle of the arm was selected to maximize the exposure on the full robotic arm.

Figure 16 shows the results of the hot case. The successful cold case is omitted in the scope of this paper. The correlation between the thermal model and the hardware was successfully achieved.

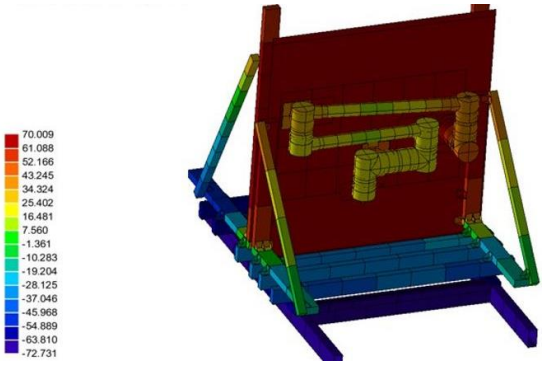

Figure 16: Hot case thermal balance testing results.

The robotic arm was also tested in a thermal vacuum environment to demonstrate that the unit withstands the environment that it is going to experience during the mission life, and to evaluate its functional performance under these conditions in a configuration shown in Figure 12. All tests were successful, and functionality was showcased at different levels of the cycle. The next step is system level functional and performance testing on the robotic test stand shown in Figure 17.

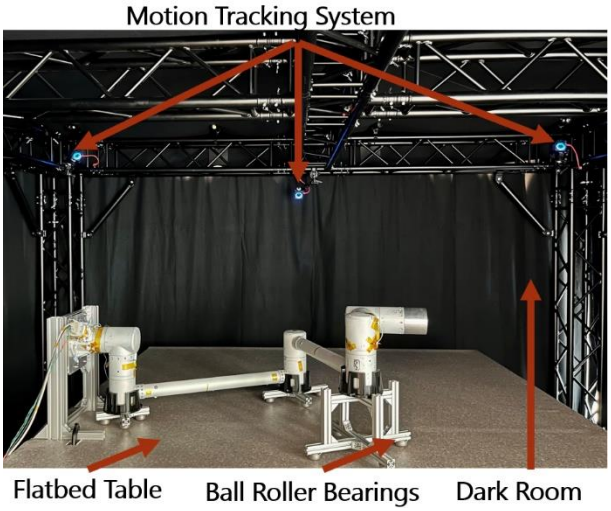

Figure 17: Robotic test stand.

6. CONCLUSION

The main lessons learned from the design and qualification of the STAARK system are:

- The 1G capability requires sizing and input sensors that are a significant cost driver. As such, it is critical to identify whether it is a critical qualification and implementation requirement for the specific mission.
- In our case passive HDRM appears to not be a viable solution and does not improve the structural performance during vibration.
- Procured additional test-boards for software development need to be provisioned.
- The major trade-off during development has been a higher system complexity through fault mitigation strategies versus high reliability component costs.
- Trusted suppliers, partners, and parts are required to streamline procurement due to long lead-times.

Finally, the next steps that Redwire has planned are:

- Implementation of input sensor for increased torque and speed margins. Completion of qualification tests

(EMI/EMC, Lifetime, System level performance testing).
- Development of a second smaller joint size to reduce mass on the wrist.
- Implementation of advanced capabilities & software qualification.

A special thank you to the Luxembourg Space Agency for funding the STAARK program and the European Space Agency Automation & Robotics team for guidance and technical supervision.

7. REFERENCES

[1] GVR. (2020). Space Robotics Market Size, Share & Trends Analysis Report. Report ID: GVR-4-68038-256-3. (115 pages)

[2] Dubowsky, S., & Papadopoulos, E. (1993). The kinematics, dynamics, and control of free-flying and free-floating space robotic systems. IEEE Transactions on Robotics and Automation, 9(5), 531-543. doi: 10.1109/70.258046.

[3] Barada, K. R., Martinez, C., Dentler, J., Olivares Mendez, M. A. (2021). Towards Incremental Autonomy Framework for On-Orbit Vision-Based Grasping. In 72nd International Astronautical Congress, Dubai, United Arab Emirates, 25-29 October 2021.